Treg-expressed CTLA-4 depletes CD80/CD86 by trogocytosis, releasing free PD-L1 on antigen-presenting cells

Murat Tekguc[a], James Badger Wing[a,b], Motonao Osaki[a,c], Jia Long[a], and Shimon Sakaguchi[a,c,1]

[a]Laboratory of Experimental Immunology, World Premier International (WPI) Immunology Frontier Research Center (IFReC), Osaka University, Suita 565-0871, Japan; [b]Laboratory of Human Immunology (Single Cell Immunology), WPI IFReC, Osaka University, Suita 565-0871, Japan; and [c]Department of Experimental Pathology, Institute for Frontier Medical Sciences, Kyoto University, Kyoto 606-8507, Japan

Contributed by Shimon Sakaguchi, June 22, 2021 (sent for review November 16, 2020; reviewed by Miyuki Azuma and Megan K. Levings)

Foxp3-expressing CD4$^+$CD25$^+$ regulatory T cells (Tregs) constitutively and highly express the immune checkpoint receptor cytotoxic T-lymphocyte-associated antigen-4 (CTLA-4), whose Treg-specific deficiency causes severe systemic autoimmunity. As a key mechanism of Treg-mediated suppression, Treg-expressed CTLA-4 down-regulates the expression of CD80/CD86 costimulatory molecules on antigen-presenting cells (APCs). Here, we show that Treg-expressed CTLA-4 facilitated Treg-APC conjugation and immune synapse formation. The immune synapses thus formed provided a stable platform whereby Tregs were able to deplete CD80/CD86 molecules on APCs by extracting them via CTLA-4–dependent trogocytosis. The depletion occurred even with Tregs solely expressing a mutant CTLA-4 form lacking the cytoplasmic portion required for its endocytosis. The CTLA-4–dependent trogocytosis of CD80/CD86 also accelerated in vitro and in vivo passive transfer of other membrane proteins and lipid molecules from APCs to Tregs without their significant reduction on the APC surface. Furthermore, CD80 down-regulation or blockade by Treg-expressed membrane CTLA-4 or soluble CTLA-4-immunoglobulin (CTLA-4-Ig), respectively, disrupted cis-CD80/programmed death ligand-1 (PD-L1) heterodimers and increased free PD-L1 on dendritic cells (DCs), expanding a phenotypically distinct population of CD80^{lo} free PD-L1^{hi} DCs. Thus, Tregs are able to inhibit the T cell stimulatory activity of APCs by reducing their CD80/CD86 expression via CTLA-4–dependent trogocytosis. This CD80/CD86 reduction on APCs is able to exert dual suppressive effects on T cell immune responses by limiting CD80/CD86 costimulation to naïve T cells and by increasing free PD-L1 available for the inhibition of programmed death-1 (PD-1)–expressing effector T cells. Blockade of CTLA-4 and PD-1/PD-L1 in combination may therefore synergistically hinder Treg-mediated immune suppression, thereby effectively enhancing immune responses, including tumor immunity.

CTLA-4 | trogocytosis | regulatory T cells | CD80/CD86 | PD-L1

Regulatory T cells (Tregs), which express Foxp3 as a lineage-specific transcription factor, play a crucial role in the maintenance of immunological self-tolerance and homeostasis (1). Tregs highly and constitutively express cytotoxic T-lymphocyte-associated antigen-4 (CTLA-4) (2–4), which is essential for Treg-mediated immunosuppressive function. In vivo blockade of CTLA-4 by specific antibodies elicited autoimmune diseases in mice similar to those induced by Treg deficiency (4). Furthermore, Treg-specific deletion of CTLA-4 in mice evoked systemic autoimmune/inflammatory disease (5). Treg-specific CTLA-4 deficiency or its blockade also disrupted in vitro Treg-mediated suppression (4–6). In addition to these experimental findings, patients with CTLA-4 haploinsufficiency developed systemic autoimmunity most likely due to impaired Treg-suppressive function (7, 8). Mechanistically, Tregs are able to down-regulate in vitro the expression of CD80/CD86 by antigen-presenting cells (APCs) in a CTLA-4–dependent manner, thereby hindering the activation of conventional T cells (Tconvs) (5, 6, 9). This cell-extrinsic function of CTLA-4 has been suggested to play a dominant role in preventing autoimmunity, since bone marrow chimeric mice that harbored both CTLA-4–sufficient and –deficient T cells remained healthy (10). These findings collectively indicate a critical contribution of Treg-expressed CTLA-4 to Treg-mediated suppression, yet the precise molecular mechanism of CTLA-4–dependent Treg suppression remains obscure.

Approximately 90% of total-CTLA-4 has been estimated to cycle between the cell surface and the intracellular compartment via clathrin-mediated endocytosis regardless of CD80/CD86 binding (11). The YVKM motif in its cytoplasmic tail portion interacts with the clathrin adaptor activating protein 2 (AP-2); T cell activation phosphorylates the YVKM motif and inhibits its binding to AP-2, leading to membrane retention of CTLA-4 (12–14). Given this active intracellular CTLA-4 cycling, former studies (15, 16) demonstrated that once CTLA-4 binds to its ligands CD80/CD86, it mediates their direct endocytosis (trans-endocytosis) via its tail portion, leading to down-regulation of CD80/CD86 on APCs. On the other hand, it was previously shown that constitutive and high expression of a tailless (TL) CTLA-4, defective in endocytosis and signal transduction, was able to confer Treg-like suppressive activity on Tconv cells (17). Several studies have also shown that TL Tregs suppressed the

Significance

Immunosuppressive Tregs constitutively express CTLA-4, an immune checkpoint receptor. Addressing the role of CTLA-4 in Treg-suppressive function, we show that Treg-expressed CTLA-4, even in the absence of its cytoplasmic portion, promoted the conjugation of Tregs and antigen-presenting cells (APCs), leading to CTLA-4–dependent trogocytosis of CD80/CD86 and concomitant transfer of membrane fragments from APCs to the Treg cell surface. The depletion or blockade of CD80 by trogocytosis or solubilized CTLA-4, respectively, increased free PD-L1 by disrupting cis-CD80/PD-L1 heterodimers on APCs. Thus, Tregs can exert dual suppressive effects through the limitation of CD80/CD86 and up-regulation of free PD-L1 on APCs. Cancer immunotherapy with anti–CTLA-4 and anti–PD-1/PD-L1 blocking antibodies may enhance tumor immunity by hindering this Treg-mediated immune suppression.

Author contributions: M.T., J.B.W., M.O., and S.S. designed research; M.T. performed research; M.O. contributed new reagents/analytic tools; M.T., J.L., and S.S. analyzed data; and M.T., J.B.W., and S.S. wrote the paper.

Reviewers: M.A., Tokyo Medical and Dental University; and M.K.L., The University of British Columbia.

Competing interest statement: Authors S.S., J.B.W., and the reviewer M.K.L. contributed independently as coauthors to guideline mega-studies, which were published as A. Cossarizza et al., *Eur. J. Immunol.* **47**, 1584–1797 (2017); A. Fuchs et al., *Front. Immunol.* **8**, 1–15 (2018); and A. Cossarizza et al., *Eur. J. Immunol.* **49**, 1457–1973 (2019).

[1]To whom correspondence may be addressed. Email: shimon@ifrec.osaka-u.ac.jp.

This article contains supporting information online at https://www.pnas.org/lookup/suppl/doi:10.1073/pnas.2023739118/-/DCSupplemental.

Published July 23, 2021.

proliferation of Tconvs as efficiently as wild-type (WT) Tregs (18, 19), whereas others suggested that transgenic TL Tregs displayed defective suppressive function (20). It thus needs to be determined how CTLA-4 precisely mediates the cell-extrinsic suppressive function of Tregs.

Accumulating evidence indicates that CD80 not only interacts, in trans, with CD28 and CTLA-4 expressed on T cells but also, in cis, with programmed death ligand-1 (PD-L1) protein expressed by APCs (21, 22). These cis-CD80/PD-L1 heterodimers on APCs limit the availability of free PD-L1, thereby interfering with the transbinding between PD-L1 and its receptor PD-1 expressed on T cells (23, 24). It can be asked then whether Treg-expressed CTLA-4 is able to control the availability of PD-L1 through modulating CD80 expression on APCs.

In this report, we have addressed the molecular mechanism of CTLA-4–dependent Treg suppression and shown that Tregs down-regulate CD80/CD86 expression on APCs via CTLA-4–dependent trogocytosis. This CD80/CD86 down-regulation results in up-regulation of free PD-L1 expression on APCs. In combination, these events enable Tregs to suppress not only naïve Tconvs, but also activated PD-1–expressing effector Tconvs.

Results

Tregs Uptake CD80/CD86 and Accompanying Membrane Fragments of APCs by CTLA-4–Dependent Trogocytosis. In order to determine the role of the cytoplasmic tail portion of CTLA-4 in its cell-extrinsic function, we used tailless (TL) CTLA-4 transgenic (TLC4Tg) mice, whose T cells expressed a mutant CTLA-4 protein without its cytoplasmic tail portion (17, 25). To obtain Tregs expressing solely TL CTLA-4, TLC4Tg mice were backcrossed to BALB/c CTLA-4 full knockout (KO) mice and made deficient in endogenous CTLA-4 (17). For functional comparison with TL Tregs, CTLA-4 KO and WT CTLA-4–expressing Tregs were isolated from female CTLA-$4^{flox/flox}$, $Foxp3^{IRES\text{-}Cre}$ heterozygous, Rosa-RFP-reporter (CRF) mice on the BALB/c background, which harbored both WT and KO Tregs without developing spontaneous autoimmunity (5, 26). Using such Treg populations purified as $CD4^+CD25^+$ T cells (>95% $Foxp3^+$ by intracellular Foxp3 staining), TL Tregs abundantly expressed both cell surface and intracellular CTLA-4, whereas a majority of CTLA-4 was localized intracellularly in WT Tregs (Fig. 1 *A*, *Upper*). Previous studies showed that the tail portion of CTLA-4 was indispensable for its intracellular trafficking and transendocytosis function (12–15). To assess the endocytic function of TL CTLA-4, we first labeled the cycling and noncycling CTLA-4 on Treg cell surface at 37 °C and then tagged the noncycling CTLA-4 by a secondary antibody at 4 °C, which revealed single- and double-stained CTLA-4 as cycling and noncycling CTLA-4, respectively (27) (Fig. 1 *A*, *Lower*). This assay confirmed that the whole population of TL CTLA-4 was retained on the cell membrane and lacked cycling ability (single-stained CTLA-4/total-CTLA-4 = 0.2%), in contrast to WT CTLA-4, most of which were detected as cycling (single-stained CTLA-4/total-CTLA-4 = 86.3%).

For tracking the CD80/CD86 molecules expressed on the dendritic cell (DC) surface following their interaction with Tregs, we generated three types of gene-transduced murine DC lines: JAWSII cells expressing CD80-GFP or CD86-GFP fusion protein or GFP alone (abbreviated as 80-JAWSII, 86-JAWSII, and GFP-JAWSII cells, respectively). While GFP-JAWSII DCs expressed a low quantity of endogenous CD80 and CD86, 80-JAWSII and 86-JAWSII DCs expressed much higher amounts of the respective fusion proteins (Fig. 1*B*). By coculturing JAWSII DCs with ex vivo purified Tregs in various combinations (Fig. 1*C*), we assessed the uptake of CD80- or CD86-GFP fusion proteins, integrin CD11b, and DiD dye-labeled membrane lipids from the DC surface by TL, KO, or WT Tregs, which could be distinguished from JAWSII DCs by cell size and by the expression of CD4 and CD25 (*SI Appendix*, Fig. S1*A*). TL as well as WT Tregs acquired both CD80-GFP and CD86-GFP, but not GFP alone, from respective DCs, much more efficiently than KO Tregs (Fig. 1*D*). Similarly, TL and WT Tregs acquired lipophilic DiD dye (Fig. 1*E*) and CD11b protein (Fig. 1*F*) from 80- and 86-JAWSII DCs significantly more than KO Tregs, suggesting passive capture of cell membrane components in a CTLA-4–dependent fashion. These results indicate that CTLA-4–dependent uptake of CD80/CD86 and concomitant membrane fragments of DCs was mediated by trogocytosis, which is defined as the intercellular transfer of cell membrane proteins and concomitant lipid particles initiated by particular receptor–ligand interactions between donor and recipient cells (28, 29).

While CTLA-4–driven trogocytosis of CD80/CD86 was more prominent with Tregs cocultured with 80- or 86-JAWSII DCs, TL Tregs were also able to gain DiD dye and CD11b from GFP-JAWSII DCs when compared with KO Tregs (Fig. 1 *E* and *F*), which could be attributed to the endogenous expression of low amounts of CD80/CD86 by GFP-JAWSII cells (Fig. 1*B*). In addition, when a mixture of RFP-tagged KO Tregs and nontagged WT Tregs prepared from CRF mice was cocultured with 80-JAWSII DCs, WT Tregs captured much greater amounts of DC membrane fragments (CD80-GFP, CD11b, and lipophilic dye) compared with KO Tregs (*SI Appendix*, Fig. S1*B*), further supporting the CTLA-4 dependency of the transfer. Time-course kinetics of trogocytosis also revealed that Tregs could uptake CD80-GFP accompanied by passive CD11b transfer from the DC membrane in a CTLA-driven fashion even after 1 h of coincubation with 80-JAWSII DCs (*SI Appendix*, Fig. S1*C*). Moreover, CTLA-4–dependent trogocytosis could still occur even in the absence of anti-CD3e polyclonal stimulation during the overnight coculture, which suggested that allostimulation by JAWSII DCs (derived from C57BL/6 mice) was sufficient for Tregs to perform CTLA-4–mediated trogocytosis (*SI Appendix*, Fig. S1*D*).

In Treg coculture with B cells as another population of APCs, it was difficult to distinguish between CD80/CD86 molecules endogenously expressed by Tregs and those uptaken from activated B cells highly expressing CD80/CD86 (*SI Appendix*, Fig. S2*A*). Nevertheless, Tregs showed uptake of other B cell surface markers, such as CD45R, CD40, and class II MHC (MHC-II) proteins (*SI Appendix*, Fig. S2*B*). TL Tregs were higher than WT Tregs in the degree of this passive transfer and much higher than KO Tregs. In addition, the higher the ratios of B cells to Tregs, the higher was the quantity of the proteins captured by Tregs (*SI Appendix*, Fig. S2 *B*, *Lower*). Similar to JAWSII DCs, with primary mouse bone marrow-derived dendritic cells (BMDCs) (*SI Appendix*, Fig. S3 *A* and *B*) or splenic DCs (*SI Appendix*, Fig. S3 *C* and *D*), we observed CTLA-4–driven passive uptake of CD11b and CD11c molecules by cocultured WT and TL Tregs.

Taken together, Tregs are able to concomitantly acquire CD80/CD86 and other membrane proteins and lipids from DCs and B cells by CTLA-4–dependent trogocytosis, without a need of direct internalization via endocytosis that requires the CTLA-4 tail portion.

CTLA-4 Promotes Conjugate Formation between Tregs and APCs. To determine then whether CTLA-4–dependent trogocytosis might result from the stable conjugation between Tregs and APCs, we examined the contribution of CTLA-4 to the formation of Treg-DC conjugates, which could be defined as $CD4^+CD11b^+$ doublets by flow cytometric analysis (Fig. 2*A*). TL Tregs formed significantly more conjugates with 80- or 86-JAWSII DCs compared to WT or KO Tregs. They also showed a smaller, but still significant increase in their attachment to GFP-JAWSII DCs compared with KO Tregs (Fig. 2*B*), presumably due to the endogenous CD80/CD86 expression by GFP-JAWSII cells (Fig. 1*B*). Furthermore, WT Tregs generated higher percentages of conjugates than KO Tregs, especially when they were cocultured with 80-JAWSII DCs (Fig. 2 *A* and *B*). Similarly, by coculturing Tregs and lipopolysaccharide (LPS)-activated B cells, $CD4^+CD45R^+$

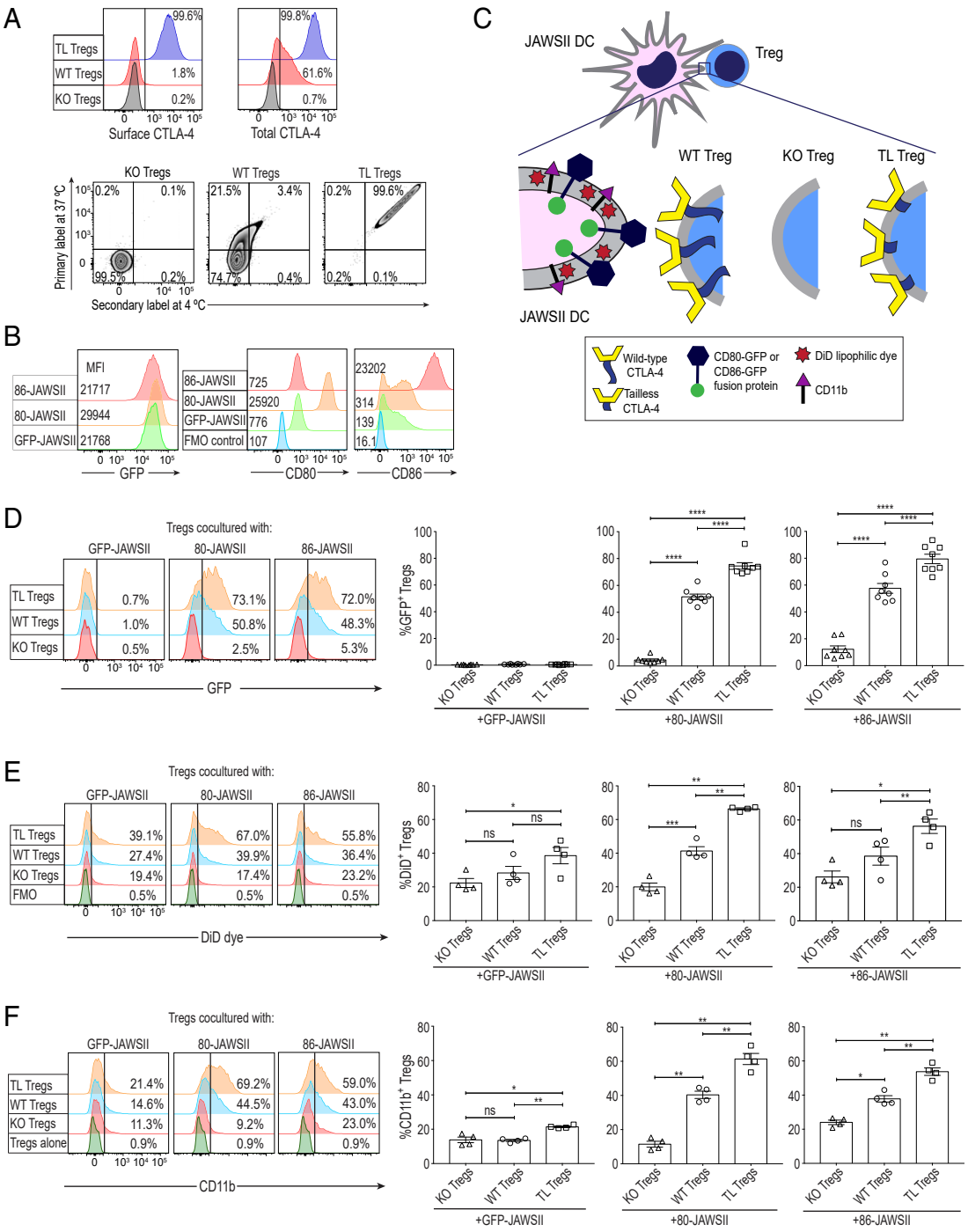

Fig. 1. Uptake of CD80/CD86 proteins and accompanying DC membrane fragments by Tregs via CTLA-4–dependent trogocytosis. (*A*) Expression and cycling patterns of Treg-expressed CTLA-4. (*Upper*) Live/Dead-dye$^-$CD4$^+$CD25$^+$Foxp3$^+$ cells were stained separately for surface and total-CTLA-4 at 4 °C. (*Lower*) Single-stained Tregs solely with the primary antibody represent the cycling CTLA-4 at 37 °C while Tregs labeled with both primary and secondary antibodies at 4 °C display the noncycling surface CTLA-4. KO and WT Tregs were purified from the spleens and peripheral lymph nodes of the same female CTLA-4$^{flox/flox}$, Foxp3$^{IRES\text{-}Cre}$ heterozygous, and Rosa-RFP-Cre reporter mice while TL Tregs were simultaneously sorted from female TLC4Tg mice. The mice used were all on the BALB/c background. Data are representative of two independent experiments. (*B*) GFP, CD80, and CD86 expression of GFP-, 80-, and 86-JAWSII DCs. A total of 5×10^4 JAWSII DCs (on the C57BL/6 background) were stimulated in the presence of 0.1 μg/mL LPS at 37 °C for 20 h. Data are representative of four independent experiments. (*C*) Experimental illustration for Treg-JAWSII DC coculture assays. GFP-, 80-, or 86-JAWSII DCs (3×10^4), labeled with lipophilic DiD dye, were incubated at a 1:2 ratio with purified KO, WT, or TL Tregs in the presence of anti-CD3e (0.5 μg/mL), IL-2 (100 IU), GM-CSF (5 ng/mL), and LPS (0.1 μg/mL) at 37 °C for 20 h. Cocultured Tregs were pregated on single Live/Dead-dye$^-$CD4$^+$CD25$^+$ cells. Transfer of proteins and lipids by Tregs from DCs was based on Treg expression of GFP, DiD dye, and CD11b. (*D*) Uptake of CD80- or CD86-GFP fusion protein by Tregs ($n = 8$). (*E*) Uptake of lipophilic DiD dye by Tregs from labeled JAWSII DCs ($n = 4$). Fluorescence minus one (FMO) staining control displays WT Tregs cultured with unlabeled JAWSII DCs. (*F*) Uptake of DC surface protein CD11b by Tregs ($n = 4$). The staining control shows WT Tregs incubated alone. Histogram in *D* is representative of eight independent experiments; histogram in *E* and *F* of four independent experiments. Numbers on histograms in *A* and *D*–*F* show the percent positive values. Means ± SEM. Asterisks indicate *P* values derived from one-way ANOVA with Tukey's multiple comparisons test (*$P \le 0.05$, **$P \le 0.01$, ***$P \le 0.001$, ****$P \le 0.0001$); ns, not significant.

(Treg-B cell) doublets were formed (Fig. 2*C*). Both TL and WT Tregs were able to generate significantly higher percentages of conjugates than KO Tregs at high Treg-to-B cell ratios in the coculture (Fig. 2*D*).

These results collectively indicate that increased availability of CTLA-4, as is the case of TL Tregs highly expressing CTLA-4, as well as its ligands, especially CD80, augments the formation of conjugates between Tregs and APCs.

CTLA-4–Dependent Trogocytosis Follows Immune Synapse Formation between Tregs and DCs. Since CTLA-4 is one of the components of the immune synapse (30, 31), we attempted to visualize the process of CTLA-4–dependent trogocytosis at the immune synapses between Tregs and DCs. Live-cell imaging of Treg-JAWSII DC cocultures by confocal microscopy demonstrated the capture of CD80-GFP and concomitant membrane lipid particles by WT and TL Tregs, but not by KO Tregs (Fig. 3*A*). We also detected similar findings with CD86-GFP capture (*SI Appendix*, Fig. S4). In addition, WT and TL Tregs showed significantly higher frequencies of Treg-DC contacts compared to KO Tregs when cocultured with 80- or 86-JAWSII DCs (Fig. 3*B*). Static imaging of fixed Treg-JAWSII DC conjugates demonstrated that polarized CTLA-4 proteins on TL or WT Tregs colocalized with CD80- or CD86-GFP aggregates at the contact sites of JAWSII DCs and Tregs in contrast to relatively diffuse distribution of integrin LFA-1 on the Treg cell surface (Fig. 3*C* and *SI Appendix*, Fig. S4). Consecutive time-lapse imaging of fresh Treg-JAWSII DC cocultures displayed the capture of CD80-GFP by TL and WT, but not KO Tregs

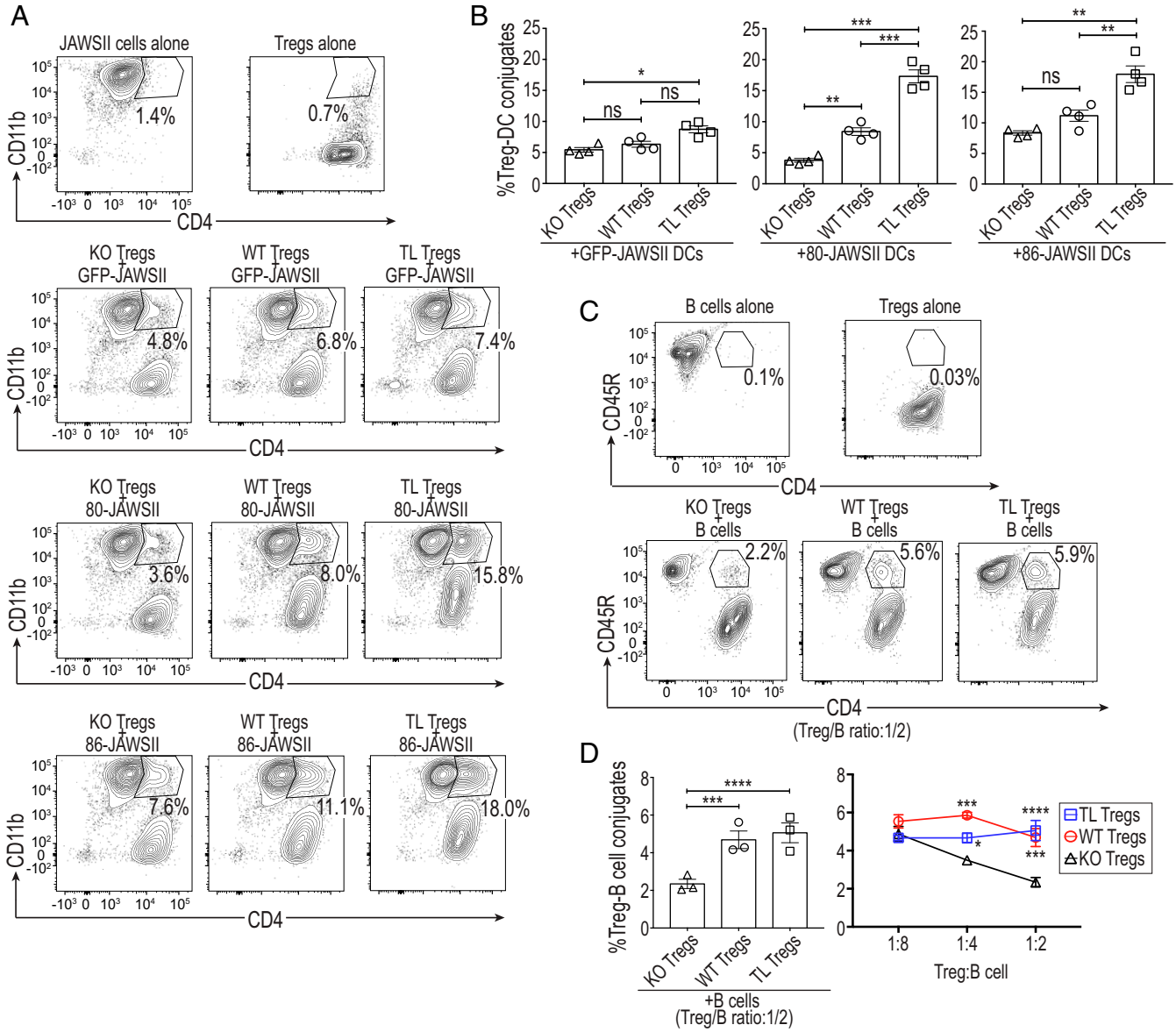

Fig. 2. CTLA-4–dependent conjugate formation of Tregs and APCs. (*A*) Formation of Treg-JAWSII DC conjugates defined as $CD4^+CD11b^+$ doublets. These doublets were pregated on total Live/Dead-dye$^-$ cells, representative of four independent experiments. GFP-, 80-, or 86-JAWSII DCs were cocultured at a 1:2 ratio for 20 h with Tregs purified from CRF and C4TLTG mice as in Fig. 1. (*B*) Summary of the quantified Treg-JAWSII conjugates ($n = 4$). (*C* and *D*) A total of 1×10^5 B cells, from WT mice, were cocultured with purified Tregs at designated ratios in the presence of anti-CD3e (0.5 μg/mL), IL-2 (100 IU), and LPS (10 μg/mL) for 72 h. (*C*) Generation of Treg-B cell conjugates defined as $CD4^+CD45R^+$ doublets pregated on total Live/Dead-dye$^-$ cells. Data are representative of three independent experiments. (*D*) Summary of the quantified Treg-B cell conjugates at various ratios ($n = 3$), from three independent experiments. Means ± SEM. Asterisks in *B* and *D* indicate *P* values derived from one-way ANOVA and two-way ANOVA with Tukey's multiple comparisons test, respectively (*$P \le 0.05$, **$P \le 0.01$, ***$P \le 0.001$, ****$P \le 0.0001$); ns, not significant.

(Movies S1–S3). These microscopic findings collectively indicate that CTLA-4–dependent trogocytosis is a key outcome of Treg-DC conjugate and immune synapse formation facilitated by the ligand-binding domain of CTLA-4, confirming the flow cytometry results.

The Tail Portion of CTLA-4 Is Dispensable for CD80/CD86 Down-Regulation on B Cells and Treg-Suppressive Function. We next examined how TL CTLA-4 on Tregs would alter the CD80/CD86 expression of activated B cells and thereby affect Treg-suppressive activity. Upon in vitro LPS stimulation, a majority of B cells became activated to express CD80/CD86 at high levels and could be distinguished from the unactivated population by cell size (Fig. 4 *A* and *B* and *SI Appendix*, Fig. S5*A*). Coculture of Tregs and these LPS-activated B cells revealed that TL Tregs were able to reduce both CD80 and CD86 expression more potently than WT Tregs at various Treg/B cell ratios, as assessed by both the median fluorescence intensity (MFI) of B cells and percentages of $CD80^+$ B cells (Fig. 4*A*) and the MFI of $CD86^+$ B cells (Fig. 4*B*). Even at a low Treg/B cell ratio (1:16), WT or TL Tregs were capable of depleting CD80 from B cells (Fig. 4*A*). In contrast, reduction of CD86 expression by WT Tregs only occurred at relatively higher Treg/B cell ratios (at 2:1 or higher) compared to TL Tregs (at 1:16 or higher) (Fig. 4*B*). While the majority of CD80 depletion was found to be CTLA-4 dependent, KO Tregs also exhibited a capacity to decrease the B cell expression of CD80 (*SI Appendix*, Fig. S5*B*), although at a much lower degree than TL or WT Tregs. Additionally, B cell expression of CD40 was reduced by Tregs, most potently by KO Tregs, while MHC-II expression was augmented by Tregs, especially by TL Tregs (*SI Appendix*, Fig. S5*B*).

In correlation with their ability to deplete CD80/CD86 on B cells, TL Tregs indeed exhibited more potent suppressive activity than WT Tregs in a Treg dose-dependent manner (Fig. 4*C*). Conversely, TL Tregs lost their superior suppressive ability compared to WT Tregs when anti-CD3/CD28 dynabeads were used to stimulate Tconv cells in the absence of APCs (*SI Appendix*, Fig. S5*C*). This finding further indicated that the suppressive ability of TL Tregs was based on CTLA-4–driven trogocytosis.

These results taken together demonstrated that in vitro Treg-suppressive activity was well correlated with CD80/CD86 down-regulation via CTLA-4–dependent trogocytosis and that the tail portion of CTLA-4 was dispensable for both. In addition, despite the ability of Tregs to uptake CD40 and MHC-II from B cells in a CTLA-4–driven manner, the effects of Tregs on B cell expression of these molecules were apparently less dependent on or independent of CTLA-4.

In Vivo Transferred Treg and Tconv Cells Passively Capture Membrane Proteins from Host Cells in a CTLA-4–Dependent Manner. Based on the above in vitro findings, we then attempted to examine whether CTLA-4–driven uptake of APC membrane proteins by Tregs might also occur in vivo. Since it was difficult to distinguish the CD80/CD86 molecules acquired by Tregs from those endogenously expressed by activated Tregs, we examined uptake of other cell surface proteins by Tregs. We transferred purified WT or KO Tregs from CD45.2 CRF mice, together with Tconvs from CD45.1 congenic mice, into syngeneic CD45.1 RAG2 KO mice, and assessed the transferred $CD45.2^+$ WT or KO Tregs for the capture of CD45.1 protein by flow cytometry 28 d later. Compared with KO Tregs, WT Tregs displayed a markedly enhanced uptake of CD45.1 surface protein from host cells. When such WT Tregs were divided into two groups according to their expression levels of CTLA-4, CTLA-4^{hi} Tregs showed significantly higher uptake of CD45.1 than CTLA-4^{lo} Tregs (Fig. 5 *A* and *B*).

Since Tconvs express CTLA-4 upon activation, we adoptively transferred $CD45.2^+$ Tconv cells into CD45.1 RAG2 KO mice to determine whether activated CTLA-4^+ Tconvs could also capture host cell-derived CD45.1 protein (Fig. 5*C*). Similar to CTLA-4–expressing Tregs, CTLA-4^+ Tconvs acquired CD45.1 protein more abundantly than CTLA-4^- Tconvs. Among CTLA-4^+ Tconvs, CTLA-4^{hi} Tconvs captured significantly more CD45.1 compared to CTLA-4^{lo} Tconvs (Fig. 5*D*).

These results collectively indicate that Tregs and activated Tconvs can uptake cell membrane proteins of the host in vivo, at least in part, by a CTLA-4–dependent mechanism.

Treg-Dependent Depletion of CD80 Increases Free PD-L1 on DCs and Converts Them into $CD80^{lo}$ Free PD-$L1^{hi}$ DCs. Earlier reports have described cis-binding of CD80 and PD-L1 on the same APCs and demonstrated that cis-CD80/PD-L1 heterodimers inhibited trans-PD-1/PD-L1 interaction through limiting the availability of CD80-unbound (free) PD-L1 to PD-1^+ T cells (22–24). Based on these findings, we investigated the effect of CTLA-4–dependent trogocytosis on cis-CD80/PD-L1 heterodimers expressed by splenic DCs. We purified $CD11c^+CD80^+$ splenic DCs from WT mice or $CD11c^+$ DCs from $CD80^{-/-}CD86^{-/-}$ double knockout (DKO) mice, both on the C57BL/6 background, and stimulated them overnight with LPS and GM-CSF to increase their CD80 and PD-L1 expression (Fig. 6*A*). We labeled DCs first with 1-111A anti–PD-L1 mAb, which was previously reported to detect total (CD80 bound and free) PD-L1 molecules (23), and then with 10F.9G2 PD-L1 mAb, which competes with CD80 for binding and stain-free PD-L1 (21, 32) (*SI Appendix*, Fig. S6*A*). 10F.9G2 mAb detected a significantly higher quantity of free PD-L1 on DKO DCs compared to WT DCs, with slightly lower staining intensity of DKO DCs by 1-111A mAb (Fig. 6 *A* and *B*). The quantification of PD-L1 mRNA in WT and DKO DCs did not reveal any significant difference between the groups, further supporting the increased staining intensity of DKO DCs by 10F.9G2 mAb was due to an increase of CD80-unbound free PD-L1 and not to enhanced PD-L1 gene expression (Fig. 6*C*). In addition, both DKO and WT DCs contained similar percentages of PD-$L2^{hi}$ cells with similar PD-L2 expression levels (Fig. 6*D*).

We then tested whether CD80 depletion by CTLA-4–dependent trogocytosis could change the availability of free PD-L1 expressed by DCs. Overnight stimulation of freshly purified splenic $CD11c^+CD80^+$ DCs from WT BALB/c mice with LPS and GM-CSF induced three fractions distinctly defined by their expression of CD80 and free PD-L1 (detected by 10F.9G2 mAb): $CD80^{hi}$ free PD-$L1^{int}$ DCs (fraction A), $CD80^{lo}$ free PD-$L1^{hi}$ DCs (fraction B), and $CD80^{lo}$ free PD-$L1^{lo}$ DCs (fraction C) (Fig. 6*E*). Coculture of DCs with WT or TL Tregs, especially with the latter, resulted in an increase in the ratios of fractions B and C and a decrease of fraction A, compared to coculture with KO Tregs (Fig. 6 *E* and *F*). Both fractions A and B were total-PD-$L1^{hi}$, fraction C being total-PD-$L1^{lo}$ (Fig. 6*E* and *SI Appendix*, Fig. S6*B*). Indeed, the ratio of free PD-$L1^{hi}$ DCs among total-PD-$L1^{hi}$ DCs increased in the presence of WT or TL Tregs (Fig. 6*G*). Staining of Treg-cocultured DCs for CD80 and total-PD-L1, PD-L2, or MHC-II showed reduction in the ratios of total-PD-$L1^{hi}$, PD-$L2^{hi}$, and MHC-II^{hi} $CD80^{hi}$ DCs, mainly due to diminution of fraction A, and a reciprocal increase in total-PD-$L1^{lo}$, PD-$L2^{lo}$, and MHC-II^{lo} $CD80^{lo}$ DCs corresponding to fraction C (Fig. 6*E* and *SI Appendix*, Fig. S6*B*). The ratios of PD-$L2^{hi}$ DCs and MHC-II^{hi} DCs increased in fraction B presumably because of conversion of fraction A to fraction B (*SI Appendix*, Fig. S6*B*).

Taken together, Tregs reduce, in a CTLA-4–dependent manner, the proportion of $CD80^{hi}$ total-PD-$L1^{hi}$ free PD-$L1^{int}$ DCs, apparently converting them into phenotypically distinct $CD80^{lo}$ total-PD-$L1^{hi}$ free PD-$L1^{hi}$ DCs, which also include PD-$L2^{hi}$ and MHC-II^{hi} DCs. CTLA-4–expressing Tregs additionally increase the proportion of $CD80^{lo}$ total/free PD-$L1^{lo}$ DCs, which are PD-$L2^{lo}$ and MHC-II^{lo}.

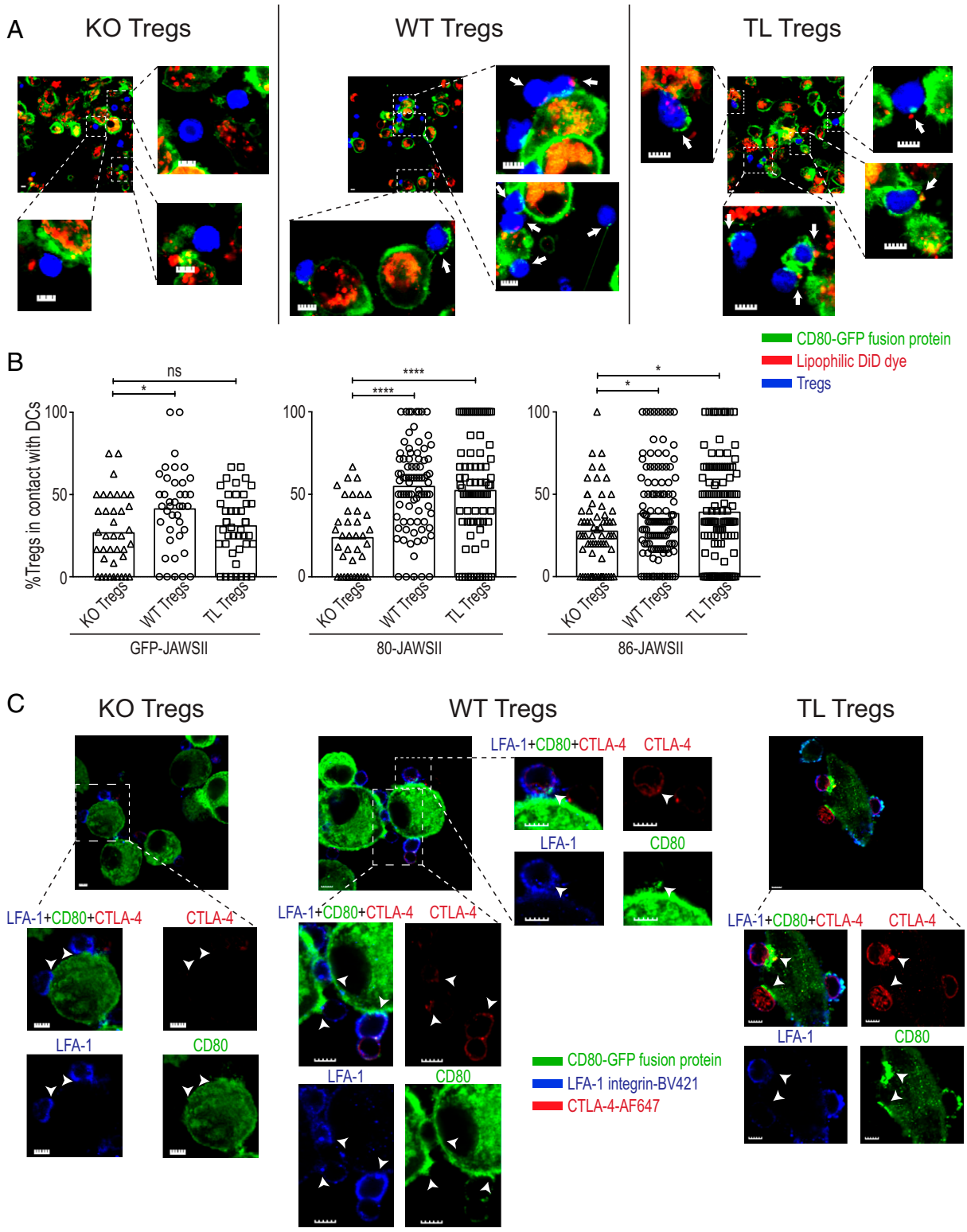

Fig. 3. Visualization of Treg-DC immune synapses as platforms for CTLA-4–dependent trogocytosis. (*A*) Live-cell imaging of Treg-JAWSII DC conjugates by confocal microscopy. Purified Tregs (prepared as shown in Fig. 1) and stained with cytoplasmic CellTracker blue dye, were incubated at a 1:1 ratio with the DiD dye-labeled JAWSII DCs (5×10^4) for 16 h. White arrows in the representative slides show the capture of CD80-GFP and/or lipid particles by Tregs prepared as shown in Fig. 1. (Scale bar, 5 μm.) (*B*) Enumeration of the contacts between Tregs and JAWSII DCs. Each symbol in the graphs denotes the ratio of Tregs, in contact with DCs, among the whole Treg population per slide (0.01 mm^2). Data are pooled from four mice, representative of four independent experiments. Asterisks indicate *P* values derived from one-way ANOVA with Tukey's multiple comparisons test (*$P \leq 0.05$, ****$P \leq 0.0001$); ns, not significant. (*C*) Colocalization of polarized CTLA-4 with CD80-GFP aggregates at Treg-JAWSII DC contact sites. Sorted WT, KO, and TL Tregs (5×10^4 cells) were cocultured at a 2:1 ratio with JAWSII DCs for 16 h. CTLA-4 (red) and LFA-1 (blue) were labeled by antibody staining following the fixation of cells. The white arrowheads mark the contact sites of JAWSII DCs and Tregs. Data are representative of two independent experiments. (Scale bar, 5 μm.)

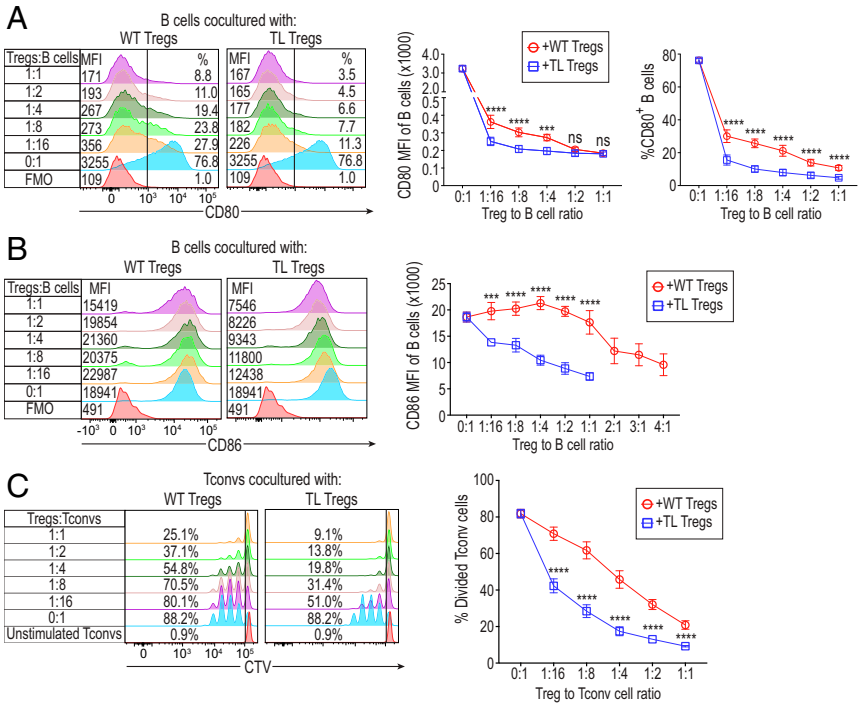

Fig. 4. In vitro Treg-suppressive activity correlated with the degree of CD80/CD86 deprivation from B cells as APCs. (*A*) Expression of CD80 by LPS-activated B cells cultured with TL or WT Tregs at various ratios. Numbers on histograms display both CD80 MFI of B cells (*Left*) and the percentages of $CD80^+$ B cells (*Right*) ($n = 4$). TL or WT Tregs from TLC4Tg or WT mice, prepared as shown in Fig. 1, were incubated with B cells (1×10^5/well) at varying ratios in the presence of anti-CD3e, IL-2, and LPS for 72 h. LPS-activated B cells were pregated on single Live/Dead-dye$^-$CD4$^-$CD45R$^+$ cells. (*B*) Expression of CD86 by LPS-activated B cells cultured with TL or WT Tregs at various ratios as shown in *A*. Numbers on histograms display CD86 MFI of B cells ($n = 4$). Data in *A* and *B* are representative of four independent experiments. (*C*) Suppressive capacity of TL and WT Tregs. A total of 1×10^5 $CD4^+$ Tconvs labeled with CellTrace Violet (CTV) dye and the same number of B cells were cocultured with purified TL or WT Tregs at various Treg/Tconv ratios in the presence of anti-CD3e (0.5 μg/mL) for 72 h. Numbers on histograms show the percentages of divided Tconv cells ($n = 4$), representative of four independent experiments. Means ± SEM. Asterisks indicate *P* values derived from two-way ANOVA with Sidak's multiple comparisons test (***$P \leq 0.001$, ****$P \leq 0.0001$); ns, not significant.

In Vitro Blockade of CD80 by CTLA-4-Ig Increases Free PD-L1 on Splenic DCs. We next addressed whether not only CD80 deprivation by CTLA-4–dependent Treg trogocytosis, but also CD80 blockade by soluble CTLA-4 would similarly up-regulate free PD-L1 on DCs. The treatment of LPS-stimulated $CD11c^+CD80^+$ splenic DCs with CTLA-4-Ig fusion protein indeed increased the level of free PD-L1 expression and the proportion of free $PD\text{-}L1^{hi}$ DCs (corresponding to fraction B in Fig. 6*E*) in a CTLA-4-Ig dose-dependent manner without altering PD-L1 mRNA expression levels (Fig. 7 *A*–*D*). The up-regulation was not observed in similarly treated DKO DCs or WT DCs treated with anti-CD80 or anti-CD86 mAb (*SI Appendix*, Fig. S7*A* and Fig. 7 *B* and *C*). The CTLA-4-Ig treatment slightly reduced the proportion of $PD\text{-}L2^{hi}$ DCs (Fig. 7*E*), as observed with WT DCs cocultured with Tregs (Fig. 6*E* and *SI Appendix*, Fig. S6*B*). This PD-L2 down-regulation did not occur in similarly treated DKO DCs or WT DCs treated with anti-CD80 or anti-CD86 mAb (*SI Appendix*, Fig. S7*B* and Fig. 7*E*). It was also noted that, upon DC activation by GM-CSF and LPS, the $CD80^{lo}$ free $PD\text{-}L1^{lo}$ fraction (corresponding to fraction C in Fig. 6*E*) was very small in proportion ($CD80^{lo}$ free $PD\text{-}L1^{lo}$ fraction was ~1% of WT DCs and $CD80^-$ free $PD\text{-}L1^{lo}$ fraction was ~5% in DKO DCs) in C57BL/6 mice used in Fig. 6 *A*–*D* and Fig. 7, compared with BALB/c mice in Fig. 6 *E*–*G*, presumably because of a genetic variation in the maturation of DCs (33, 34). Collectively, these results indicated that the increase in free PD-L1 on DCs by CTLA-4-Ig was due to the disruption of cis-CD80/PD-L1 binding.

Discussion

Naturally occurring $Foxp3^+CD25^+CD4^+$ Tregs utilize multiple humoral and cell-contact–dependent suppressive mechanisms, to control immune responses (35, 36). Among them, the CTLA-4–mediated cell-contact–dependent mechanism is crucial for Treg-mediated maintenance of immunological self-tolerance and homeostasis (5, 37). Our previous studies addressing the in vitro mechanism of Treg-mediated suppression have revealed that upon antigenic stimulation by APCs, activated Tregs physically outcompete naïve responder Tconvs to form Treg-dominant aggregates on the APCs, that this aggregate formation is LFA-1 dependent but CTLA-4 independent (6), and that the aggregated Tregs down-regulate CD80/CD86 expression on APCs in a CTLA-4–dependent manner (5, 6). We have previously shown that the first step in Treg-mediated suppression in vitro is LFA-1–dependent but CTLA-4–independent aggregation of Tregs onto APCs (6). Without LFA-1 expression by Tregs, we could not observe the aggregation or suppression of responder T cells. The present study has furthered these findings and shown CTLA-4–dependent conjugation by confocal microscopy. This suggests that following initial LFA-dependent binding, CTLA-4 plays a subsequent role in the stabilization of the Treg-APC contact and then mediates CTLA-4–dependent down-regulation of CD80/CD86. This multistep process culminating in the deprivation of CD28 costimulatory signal to naïve responder Tconvs, not only suppresses their activation, but also determines their cell fate (i.e., cell death by apoptosis, anergy, or dormancy), depending on their TCR affinity for the antigen/MHC-II complexes presented by the CD80/CD86-depleted APCs (38).

The role of the cytoplasmic signaling portion of CTLA-4 in its cell-extrinsic function has been controversial. Earlier studies showed that intracellular CTLA-4 densely accumulated at the interfaces of activated T cells and DCs in the presence of CD80

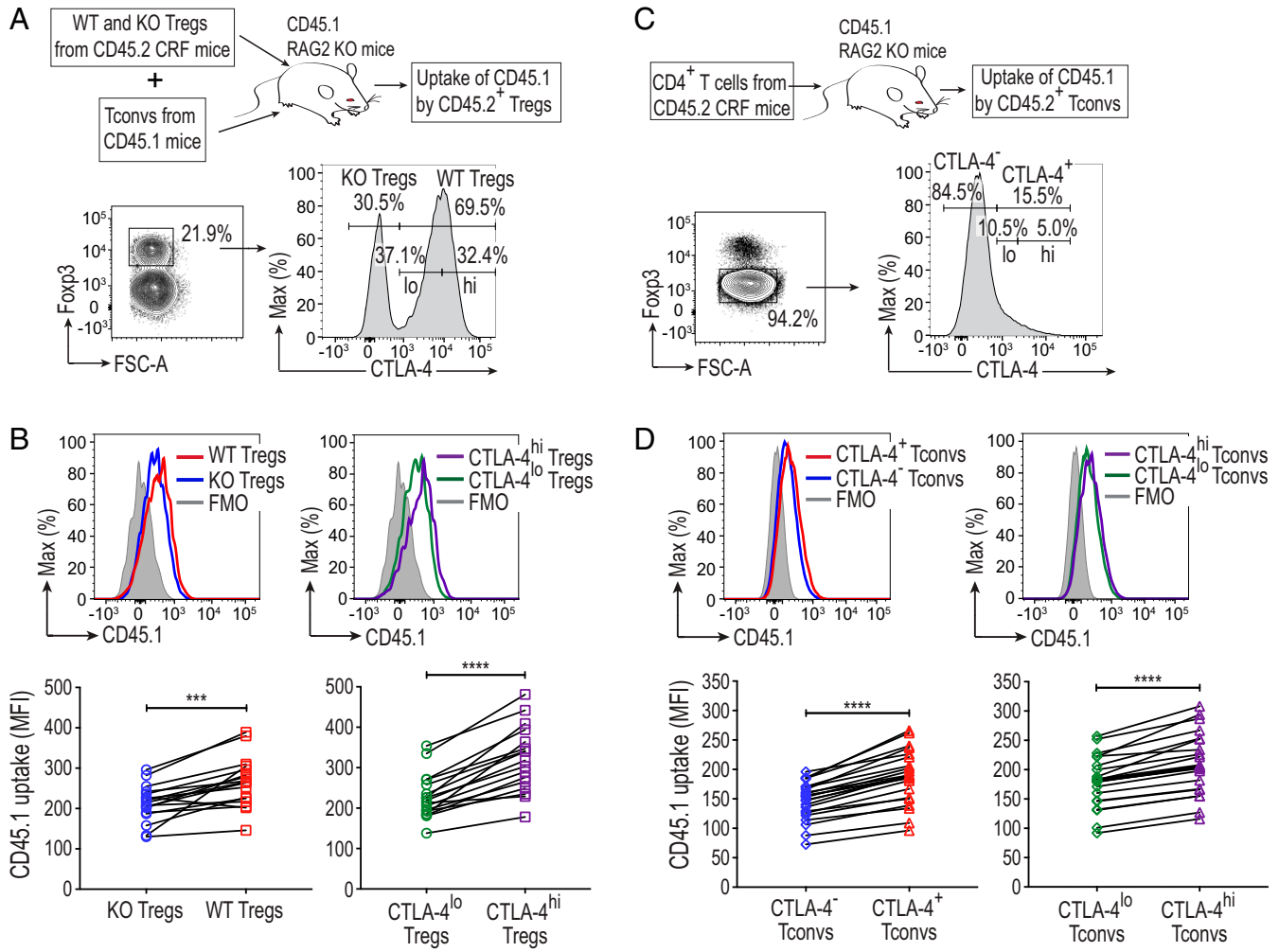

Fig. 5. Adoptively transferred Tregs and Tconvs passively acquire CD45.1 from host cells in a CTLA-4–dependent manner. (*A*) Schematic representation and the gating strategy of adoptively transferred Tregs. KO and WT Tregs (1×10^5), sorted from the same female CRF mice, were injected intravenously into CD45.1 RAG2 KO mice together with 1×10^6 $CD45R^-CD4^+CD25^-$ Tconvs from CD45.1 mice. All mice were on the BALB/c background. Spleens of the recipient mice were collected on day 28. $CD4^+$ T cells pregated as Live/Dead-dye$^-$$CD8^-CD11b^-NKp46^-CD45R^-CD11c^-CD45.2^+CD3^+CD4^+$ cells were analyzed. WT Tregs were further classified as CTLA-4^{lo} and CTLA-4^{hi} Tregs. (*B*) Uptake of CD45.1 protein by adoptively transferred Tregs. The graphs show CD45.1 MFI values of Tregs from 17 mice in three independent experiments. (*C*) Schematic representation and the gating strategy of adoptively transferred $CD4^+$ T cells. A total of 1×10^6 $CD45R^-CD4^+$ T cells purified from CRF mice were adoptively transferred intravenously into CD45.1 RAG2 KO mice and analyzed on day 28. They were classified as CTLA-4^- and CTLA-4^+ Tconvs, which were further dissected into CTLA-4^{lo} and CTLA-4^{hi} Tconvs. (*D*) Uptake of CD45.1 protein by adoptively transferred Tconvs. The graphs show CD45.1 MFI values of Tconvs from 23 mice in five independent experiments. Asterisks in *B* and *D* indicate *P* values derived from two-tailed paired *t* test (***$P \leq 0.001$, ****$P \leq 0.0001$).

(39); and blockade of CTLA-4 or its ligands disrupted the stability of Treg-DC immune synapse formation (31, 40, 41). CTLA-4 was also reported to contribute to such cell-to-cell adhesion and clustering via its cell-intrinsic signaling through Rap-1, a GTPase associated with its tail portion (42, 43). However, our confocal imaging analysis revealed a higher tendency of both WT and TL Tregs than KO Tregs to form immune synapses with DCs even in the absence of tail-associated signaling in TL Tregs. Flow cytometry analysis also supported this finding by detecting CTLA-4–dependent Treg-APC conjugate formation without the CTLA-4 tail portion in Tregs. In addition, TL Tregs, which exhibited active CTLA-4–dependent trogocytosis without the tail portion, were more potent in suppression than WT Tregs, indicating that the tail portion of CTLA-4 was dispensable for Treg-suppressive function (17, 19). Our results thus indicate that Tregs, with membrane retention of CTLA-4 upon activation (12–14), are able to suppress the proliferation of naïve Tconvs by forming CTLA-4–dependent Treg/APC conjugates and subsequently depleting its ligands CD80/CD86 from APCs, such as B cells and DCs, via CTLA-4–dependent trogocytosis.

The cell-extrinsic function of CTLA-4 was previously shown to be a one-step process called transendocytosis, which refers to direct internalization of CD80/CD86 by CTLA-4 via endocytosis (15). In contrast, our study has demonstrated that CTLA-4–dependent trogocytosis without endocytosis in Tregs is able to deprive APCs of CD80/CD86 to suppress responder T cells. It could be asked then whether high amounts of CTLA-4 retained on the cell surface of TL-Tregs might unphysiologically exaggerate the trogocytosis phenomenon. It was noted, however, that CTLA-4–dependent transfer of other membrane proteins and lipids could occur with WT Tregs, indicating physiological contribution of CTLA-4–dependent trogocytosis to CD80/CD86 deprivation from APCs. Moreover, it is plausible that CTLA-4–mediated trogocytosis of CD80/CD86 proteins to the Treg cell surface might be followed by their CTLA-4–dependent endocytosis. Supporting this notion, the ligand-binding motif of CTLA-4 is well conserved

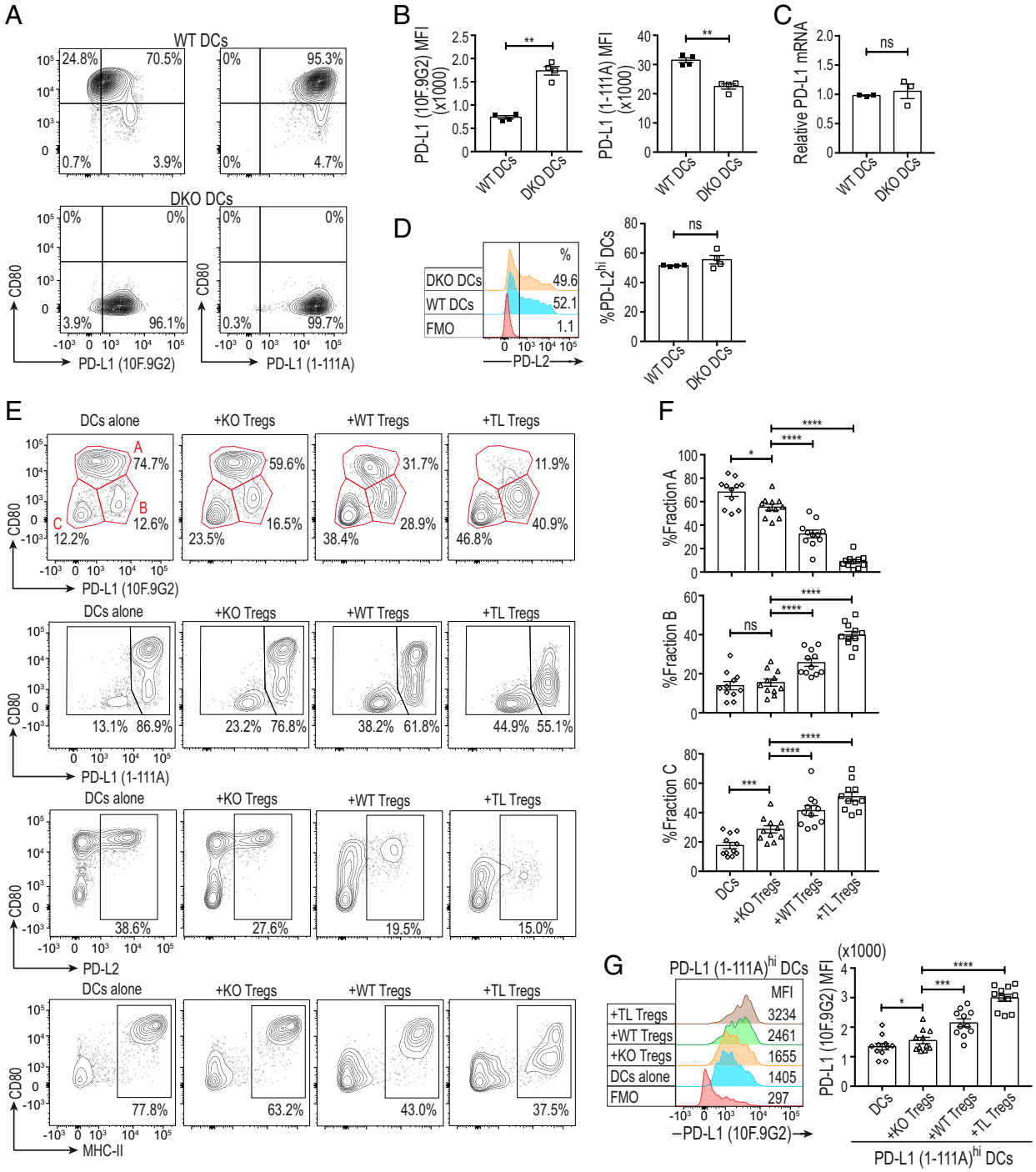

Fig. 6. Treg-dependent depletion of CD80 increases free PD-L1 on DCs and converts them into CD80^{lo} free PD-L1^{hi} DCs. (*A*) Up-regulation of free PD-L1 on CD80$^{-/-}$CD86$^{-/-}$ DKO DCs. Following the purification of CD3^{-}CD19^{-}CD11c^{+}CD80^{+} WT and CD3^{-}CD19^{-}CD11c^{+} DKO splenic DCs from WT and DKO C57BL/6 mice, respectively, 5×10^4 DCs/well were stimulated at 37 °C for 12 h in the presence of GM-CSF (10 ng/mL) and LPS (0.1 μg/mL). DCs were first labeled with biotinylated 1-111A anti–PD-L1, then stained with streptavidin, 10F.9G2 anti–PD-L1, anti–CD11c, anti–CD80, and analyzed by flow cytometry. DCs in the graphs were pregated as single Live/Dead-dye^{-}CD11c^{+} cells. (*B*) Free PD-L1 expression (revealed by 10F.9G2 anti–PD-L1 mAb) and total-PD-L1 expression (revealed by 1-111A anti–PD-L1 mAb) by WT and DKO DCs ($n = 4$). (*C*) PD-L1 mRNA expression of LPS and GM-CSF stimulated WT and DKO DCs by qRT-PCR ($n = 3$). (*D*) PD-L2 expression by WT and DKO splenic DCs. Numbers on histograms show percentages of PD-L2^{hi} DCs ($n = 4$). (*E*) CD80, free PD-L1 (10F.9G2), total-PD-L1 (1-111A), PD-L2, and MHC-II expression by splenic DCs cocultured with KO, TL, or WT Tregs. Splenic DCs (5×10^4 cells/well) purified from WT BALB/c mice as in *A* were cocultured with KO, TL, or WT Tregs (from BALB/c CRF and C4TLTG mice) at a 1:1 ratio in the presence of anti-CD3e (0.5 μg/mL), recombinant IL-2 (100 IU), GM-CSF (10 ng/mL), and LPS (0.1 μg/mL) for 12 h and then stained as in *A*. Fractions A–C in the first row were described based on the expression levels of CD80 and free PD-L1 (10F.9G2). Gating of PD-L1 (1-111A), PD-L2, and MHC-II staining indicates PD-L1 (1-111A)^{lo}/(1-111A)^{hi}, PD-L2^{hi}, and MHC-II^{hi} DCs, respectively. (*F*) The ratios of fractions A–C among DCs cocultured with KO, TL, or WT Tregs ($n = 11$). (*G*) Free PD-L1 (10F.9G2) expression by total-PD-L1 (1-111A)^{hi} DCs shown in *E* and *F*. Data in *A*–*G* are representative of two to four independent experiments. Asterisks in *B*–*D* indicate *P* values derived from two-tailed paired *t* test. Asterisks in *F* and *G* indicate *P* values derived from one-way ANOVA with Dunnett's multiple comparisons test. (*$P \le 0.05$, **$P \le 0.01$, ***$P \le 0.001$, ****$P \le 0.0001$); ns, not significant.

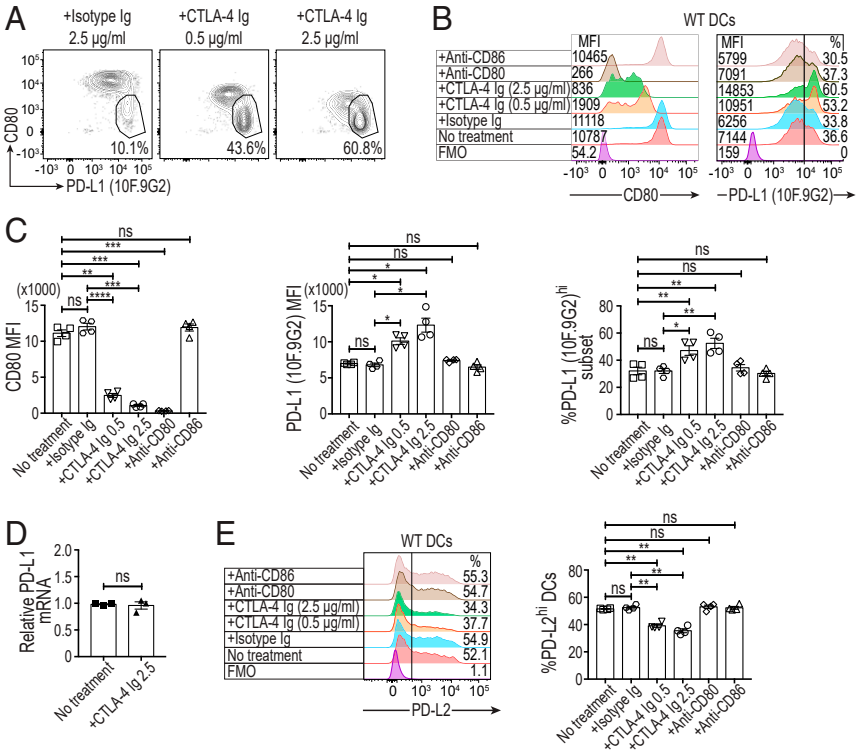

Fig. 7. Solubilized CTLA-4 releases free PD-L1 by blockade of CD80 on DCs. (*A* and *B*) The effect of CD80 blockade on free PD-L1 expression by WT splenic DCs. Numbers on the *Left* of histograms in *B* display CD80 MFI values, while percentages of free PD-L1 (10F.9G2)^{hi} DCs are shown on the *Right*. CD3$^-$CD19$^-$CD11c$^+$CD80$^+$ WT C57BL/6 splenic DCs (5×10^4 cells/well) were stimulated at 37 °C for 12 h with GM-CSF (10 ng/mL) and LPS (0.1 μg/mL) in the presence of CTLA-4 Ig, isotype Ig, anti-CD80, or anti-CD86 antibody. CTLA-4-immunoglobulin (CTLA-4-Ig) was added at the concentrations of 0.5 or 2.5 μg/mL and other antibodies at 2.5 μg/mL. The cultured DCs were stained with anti–PD-L1 (clone 10F.9G2), anti-CD11c, anti-CD80, and anti–PD-L2 for flow cytometry analysis. DCs in the graphs were pregated as single Live/Dead-dye$^-$CD11c$^+$ cells. (*C*) Summary of the effects of CD80 blockade on free PD-L1 expression by WT splenic DCs as MFIs and percentages of free PD-L1^{hi} DCs ($n = 4$). (*D*) PD-L1 mRNA expression by LPS and GM-CSF stimulated splenic DCs treated with CTLA-4 Ig ($n = 3$). (*E*) Expression of PD-L2 by WT splenic DCs treated as indicated. Numbers on histograms show percentages of PD-L2^{hi} DCs ($n = 4$). Data in *A*–*E* are representative of two independent experiments. Means ± SEM. Asterisks in *C* and *E* indicate *P* values derived from one-way ANOVA with Dunnett's multiple comparisons test. (*$P \le 0.05$, **$P \le 0.01$, ***$P \le 0.001$, ****$P \le 0.0001$); ns, not significant. *P* value in *D* is derived from a two-tailed paired *t* test.

among all vertebrates, whereas its YVKM tail motif required for endocytosis has not been conserved in fish and some amphibian species (11, 44, 45). This suggests that the process of CTLA-4 endocytosis might have emerged as an evolutionary adaptation, facilitating the clearance of bound CD80/CD86 from CTLA-4 before its recycling to the cell surface.

Earlier studies have reported that antigen-specific iTregs could suppress immune responses via TCR-mediated trogocytosis (46) that depletes peptide/MHC-II complexes from APCs, independently of CTLA-4 function (47). By using purified polyclonal Tregs, our present study has indeed demonstrated that CTLA-4–mediated trogocytosis of CD80/CD86 indirectly promoted the passive transfer of B cell and DC membrane lipids and surface proteins, such as MHC-II, CD40, CD11c, and CD11b even in the absence of anti-CD3e polyclonal stimulation. Moreover, in vivo Treg and T cell transfer experiments showed CTLA-4–driven passive capture of CD45.1 in both Tregs and activated Tconvs. In our hands, the nonspecific passive uptake of MHC-II molecules as a byproduct of CTLA-4–dependent trogocytosis did not deplete them on B cells, but rather their expression was increased. In contrast, the proportion of MHC-II^{hi} splenic DCs was decreased in Treg cocultures, while on the fraction that retained MHC-II, there was no clear change in expression level. The differences between our results and others could be, in part, attributed to their use of Tregs expressing monoclonal transgenic TCRs stimulated by a cognate peptide (47) and our use of polyclonal Tregs with polyclonal stimulation. It is possible that the depletion of both CD80/CD86 and peptide/MHC-II by trogocytosis further strengthens Treg-mediated suppression of antigen-specific Tconvs by simultaneous deprivation of costimulation and antigenic stimulation, although Tregs initially need to recognize peptide/MHC-II for their activation to exert suppression (48).

Several recent studies have shown that cis-CD80/PD-L1 heterodimers formed on APCs, especially on DCs, hinder the trans-PD-1/PD-L1 interaction by limiting the quantity of free PD-L1, thereby attenuating the inhibition of PD-1$^+$ T cells (22–24). Although a biochemical analysis showed that CTLA-4 could disrupt the cis-CD80/PD-L1 heterodimers by facilitating CD80 homodimerization (49), the impact of Treg-expressed or solubilized CTLA-4 on free PD-L1 expression by APCs has not been determined yet. Our present study demonstrated that both solubilized and Treg-expressed CTLA-4 was able to release free PD-L1 from cis-CD80/PD-L1 heterodimers on DCs by CD80 blockade or CD80 deprivation by trogocytosis, respectively. Thus, coculturing activated DCs with Tregs converted highly stimulatory CD80^{hi} free PD-L1^{int} PD-L2$^{hi\sim lo}$ MHC-II^{hi} activated DCs into two phenotypically distinct nonstimulatory/inhibitory DC populations: CD80^{lo} free PD-L1^{hi} DCs and CD80^{lo} total/free PD-L1^{lo} DCs. It remains to be determined how each DC population, expanded or reduced by Tregs, contributes to immune suppression/tolerance and homeostasis and how Tregs affect PD-L1 expression by other APCs such as B cells.

Taken together, CTLA-4–dependent Treg trogocytosis may exert a dual suppressive effect on both naïve and PD-1–expressing

activated Tconvs by limiting the CD80/CD86 costimulation and promoting the PD-L1–dependent coinhibition, respectively (*SI Appendix*, Fig. S8). Given the effectiveness of combination therapies with anti–CTLA-4 and anti–PD-1/PD-L1 for advanced stage cancers (50), our results imply that these combination therapies may strongly interfere with Treg-mediated immune suppression at both the priming and effector phases of T cell immune responses, thereby contributing to enhanced tumor immunity, albeit with occasional induction of autoimmunity.

Materials and Methods

Detailed methods are available in *SI Appendix, SI Materials and Methods* and Table S1.

Mice. BALB/c and C57BL/6 mice were purchased from CLEA Japan Inc. and maintained under specific pathogen-free conditions. All murine experiments were conducted according to the institutional guidelines for animal welfare under approved protocols by the animal experiment committee of Osaka or Kyoto University. WT and $CD80^{-/-}CD86^{-/-}$ DKO mice on the C57BL/6 background were used to purify splenic DCs. Tailless CTLA-4 transgenic (TLC4Tg) mice on the BALB/c background expressed a mutant CTLA-4, whose cytoplasmic tail portion was deleted, under the control of the human CD2 promoter as previously reported (17, 25). These mice were rendered endogenous CTLA-4 deficient by mating with BALB/c CTLA-$4^{-/-}$ mice. CTLA-$4^{flox/flox}$, $Foxp3^{IRES\text{-}Cre}$, and Rosa-RFP-Cre reporter mice (CRF mice) on the BALB/c background were previously reported (5). For Treg experiments, age- and sex-matched (female) CRF, TLC4Tg, or WT BALB/c mice were used.

Flow Cytometry Analysis. Surface and intracellular staining of cells was performed at 4 °C for 30 min and 60 min, respectively. Samples were then collected on BD LSR Fortessa and BD FACSCantoII machines with compensation and data analysis with FlowJo version 10.5.0. Median rather than mean fluorescence intensity was preferred due to its increased robustness in accordance with guidelines (51). Dead cells were separated from live cells according to their positivity for IR Live/Dead dye (Molecular Probes). Monoclonal antibodies used for the flow cytometry experiments are listed in *SI Appendix*, Table S1.

Preparation of Murine JAWSII DC Lines Expressing GFP-CD80 or GFP-CD86. First, to generate monomeric GFP, a dimer-interrupting A206K mutation was introduced into pMCs-IG (pMCs-IRES-GFP) vector by using KOD-plus-mutagenesis kit (Toyobo). CD80 and CD86 gene constructs were amplified by PCR to remove the stop codons, and a twenty-residue glycine-serine linker for each protein was designed to link them with monomeric GFP. Subsequently, gene constructs of CD80 or CD86 assembled with GFP and the linker were cloned into the modified pMCs-IG (IRES-GFP deleted) retroviral vector (52) by Gibson Assembly cloning kit (New England BioLabs). Following the transduction process of JAWSII DCs (bone marrow-derived immortalized immature dendritic cells originated from C57BL/6 mice, ATCC) with pMCs-CD80-GFP, pMCs-CD86-GFP fusion constructs, or empty pMCs-IG vector, they were further sorted several times by the BD FACSAria-SORP system based on their GFP expression, thus generating three types of JAWSII dendritic cell lines: GFP^{hi} (GFP-JAWSII), CD80-GFP^{hi} (80-JAWSII), and CD86-GFP^{hi} (86-JAWSII) DCs.

Statistics. Two-tailed paired *t* test was applied for comparing two groups for one independent variable, while two-way ANOVA assessed two groups based on two independent variables with Sidak's multiple comparisons test. The comparisons between multiple groups were calculated by one-way or two-way ANOVA with Tukey's multiple comparisons test. In addition, we compared the samples with respect to the control group by one-way ANOVA with Dunnett's multiple comparisons test. In all cases, asterisks on graphs represent significance as following ($*P \leq 0.05$, $**P \leq 0.01$, $***P \leq 0.001$, $****P \leq 0.0001$); ns, not significant. All statistical analyses were performed using GraphPad Prism V7.0e software.

Data Availability. All study data are included in the article and/or supporting information.

ACKNOWLEDGMENTS. This project was funded by the Japan Society for the Promotion of Science (JSPS) Grants-in-Aid for Specially Promoted Research (16H06295 to S.S.), Core Research for Evolutional Science and Technology of Japan Agency for Medical Research and Development (JP 19gm0010005 to S.S.), and Leading Advanced Projects for Medical Innovation (to S.S.). M.T. was supported by the Interdisciplinary Program for Biomedical Sciences Management Expenses Grant (J179913002). J.B.W. was supported by JSPS Grant-in-Aid for Scientific Research (C) (18K07175). We thank K. Suzuki and A. Nakai for providing the intracellular staining protocol for microscopy and for valuable discussion; B. Temizoz, G. Parajuli, C. Tay, and Y. Kidani for providing protocols and reagents and for helpful discussions; and Y. Kobayashi for providing $CD80^{-/-}CD86^{-/-}$ double knockout mice. We also thank Huseyin Remzi Tekguc and Serican Tekguc for their enormous support since the beginning of the project.

1. S. Sakaguchi *et al.*, Regulatory T cells and human disease. *Annu. Rev. Immunol.* **38**, 541–566 (2020).
2. S. Read, V. Malmström, F. Powrie, Cytotoxic T lymphocyte-associated antigen 4 plays an essential role in the function of CD25(+)CD4(+) regulatory cells that control intestinal inflammation. *J. Exp. Med.* **192**, 295–302, 10.1084/jem.192.2.295 (2000).
3. B. Salomon *et al.*, B7/CD28 costimulation is essential for the homeostasis of the CD4+CD25+ immunoregulatory T cells that control autoimmune diabetes. *Immunity* **12**, 431–440 (2000).
4. T. Takahashi *et al.*, Immunologic self-tolerance maintained by CD25(+)CD4(+) regulatory T cells constitutively expressing cytotoxic T lymphocyte-associated antigen 4. *J. Exp. Med.* **192**, 303–310 (2000).
5. K. Wing *et al.*, CTLA-4 control over Foxp3+ regulatory T cell function. *Science* **322**, 271–275 (2008).
6. Y. Onishi, Z. Fehervari, T. Yamaguchi, S. Sakaguchi, Foxp3+ natural regulatory T cells preferentially form aggregates on dendritic cells in vitro and actively inhibit their maturation. *Proc. Natl. Acad. Sci. U.S.A.* **105**, 10113–10118 (2008).
7. D. Schubert *et al.*, Autosomal dominant immune dysregulation syndrome in humans with CTLA4 mutations. *Nat. Med.* **20**, 1410–1416 (2014).
8. H. S. Kuehn *et al.*, Immune dysregulation in human subjects with heterozygous germline mutations in CTLA4. *Science* **345**, 1623–1627 (2014).
9. C. Oderup, L. Cederbom, A. Makowska, C. M. Cilio, F. Ivars, Cytotoxic T lymphocyte antigen-4-dependent down-modulation of costimulatory molecules on dendritic cells in CD4+ CD25+ regulatory T-cell-mediated suppression. *Immunology* **118**, 240–249 (2006).
10. M. F. Bachmann, G. Köhler, B. Ecabert, T. W. Mak, M. Kopf, Cutting edge: Lymphoproliferative disease in the absence of CTLA-4 is not T cell autonomous. *J. Immunol.* **163**, 1128–1131 (1999).
11. L. S. K. Walker, D. M. Sansom, The emerging role of CTLA4 as a cell-extrinsic regulator of T cell responses. *Nat. Rev. Immunol.* **11**, 852–863 (2011).
12. T. Shiratori *et al.*, Tyrosine phosphorylation controls internalization of CTLA-4 by regulating its interaction with clathrin-associated adaptor complex AP-2. *Immunity* **6**, 583–589 (1997).
13. E. Chuang *et al.*, Interaction of CTLA-4 with the clathrin-associated protein AP50 results in ligand-independent endocytosis that limits cell surface expression. *J. Immunol.* **159**, 144–151 (1997).
14. J. D. Bradshaw *et al.*, Interaction of the cytoplasmic tail of CTLA-4 (CD152) with a clathrin-associated protein is negatively regulated by tyrosine phosphorylation. *Biochemistry* **36**, 15975–15982 (1997).
15. O. S. Qureshi *et al.*, Trans-endocytosis of CD80 and CD86: A molecular basis for the cell-extrinsic function of CTLA-4. *Science* **332**, 600–603 (2011).
16. V. Ovcinnikovs *et al.*, CTLA-4-mediated transendocytosis of costimulatory molecules primarily targets migratory dendritic cells. *Sci. Immunol.* **4**, 1–12 (2019).
17. T. Yamaguchi *et al.*, Construction of self-recognizing regulatory T cells from conventional T cells by controlling CTLA-4 and IL-2 expression. *Proc. Natl. Acad. Sci. U.S.A.* **110**, E2116–E2125 (2013).
18. H. Kataoka *et al.*, CD25(+)CD4(+) regulatory T cells exert in vitro suppressive activity independent of CTLA-4. *Int. Immunol.* **17**, 421–427 (2005).
19. X. Tai *et al.*, Basis of CTLA-4 function in regulatory and conventional CD4(+) T cells. *Blood* **119**, 5155–5163 (2012).
20. M. Stumpf, X. Zhou, S. Chikuma, J. A. Bluestone, Tyrosine 201 of the cytoplasmic tail of CTLA-4 critically affects T regulatory cell suppressive function. *Eur. J. Immunol.* **44**, 1737–1746 (2014).
21. M. J. Butte, M. E. Keir, T. B. Phamduy, A. H. Sharpe, G. J. Freeman, Programmed death-1 ligand 1 interacts specifically with the B7-1 costimulatory molecule to inhibit T cell responses. *Immunity* **27**, 111–122 (2007).
22. A. Chaudhri *et al.*, PD-L1 Binds to B7-1 only in cis on the same cell surface. *Cancer Immunol. Res.* **6**, 921–929 (2018).
23. D. Sugiura *et al.*, Restriction of PD-1 function by cis-PD-L1/CD80 interactions is required for optimal T cell responses. *Science* **364**, 558–566 (2019).
24. Y. Zhao *et al.*, PD-L1:CD80 cis-heterodimer triggers the co-stimulatory receptor CD28 while repressing the inhibitory PD-1 and CTLA-4 pathways. *Immunity* **51**, 1059–1073.e9 (2019).
25. S. Takahashi *et al.*, In vivo overexpression of CTLA-4 suppresses lymphoproliferative diseases and thymic negative selection. *Eur. J. Immunol.* **35**, 399–407 (2005).
26. J. B. Wing, W. Ise, T. Kurosaki, S. Sakaguchi, Regulatory T cells control antigen-specific expansion of Tfh cell number and humoral immune responses via the coreceptor CTLA-4. *Immunity* **41**, 1013–1025 (2014).
27. O. S. Qureshi *et al.*, Constitutive clathrin-mediated endocytosis of CTLA-4 persists during T cell activation. *J. Biol. Chem.* **287**, 9429–9440 (2012).

28. K. A. Ahmed, M. A. Munegowda, Y. Xie, J. Xiang, Intercellular trogocytosis plays an important role in modulation of immune responses. *Cell. Mol. Immunol.* **5**, 261–269 (2008).
29. G. Li *et al*., T cell antigen discovery via trogocytosis. *Nat. Methods* **16**, 183–190 (2019).
30. J. B. Huppa, M. M. Davis, T-cell-antigen recognition and the immunological synapse. *Nat. Rev. Immunol.* **3**, 973–983 (2003).
31. W. Lin *et al*., The bullseye synapse formed between CD4+ T-cell and staphylococcal enterotoxin B-pulsed dendritic cell is a suppressive synapse in T-cell response. *Immunol. Cell Biol.* **93**, 99–110 (2015).
32. S. T. Haile, S. P. Dalal, V. Clements, K. Tamada, S. Ostrand-Rosenberg, Soluble CD80 restores T cell activation and overcomes tumor cell programmed death ligand 1-mediated immune suppression. *J. Immunol.* **191**, 2829–2836 (2013).
33. T. Liu, T. Matsuguchi, N. Tsuboi, T. Yajima, Y. Yoshikai, Differences in expression of Toll-like receptors and their reactivities in dendritic cells in BALB/c and C57BL/6 mice. *Infect. Immun.* **70**, 6638–6645 (2002).
34. X. Chen, J. J. Oppenheim, O. M. Z. Howard, BALB/c mice have more CD4+CD25+ T regulatory cells and show greater susceptibility to suppression of their CD4+CD25- responder T cells than C57BL/6 mice. *J. Leukoc. Biol.* **78**, 114–121 (2005).
35. D. A. A. Vignali, L. W. Collison, C. J. Workman, How regulatory T cells work. *Nat. Rev. Immunol.* **8**, 523–532 (2008).
36. E. M. Shevach, Mechanisms of Foxp3+ T regulatory cell-mediated suppression. *Immunity* **30**, 636–645 (2009).
37. S. Sakaguchi, K. Wing, Y. Onishi, P. Prieto-Martin, T. Yamaguchi, Regulatory T cells: How do they suppress immune responses? *Int. Immunol.* **21**, 1105–1111 (2009).
38. Y. Maeda *et al*., Detection of self-reactive $CD8^+$ T cells with an anergic phenotype in healthy individuals. *Science* **346**, 1536–1540 (2014).
39. T. Yokosuka *et al*., Spatiotemporal basis of CTLA-4 costimulatory molecule-mediated negative regulation of T cell activation. *Immunity* **33**, 326–339 (2010).
40. M. P. Matheu *et al*., Imaging regulatory T cell dynamics and CTLA4-mediated suppression of T cell priming. *Nat. Commun.* **6**, 6219 (2015).
41. N. Dilek *et al*., Targeting CD28, CTLA-4 and PD-L1 costimulation differentially controls immune synapses and function of human regulatory and conventional T-cells. *PLoS One* **8**, e83139 (2013).
42. T. J. Dillon, K. D. Carey, S. A. Wetzel, D. C. Parker, P. J. S. Stork, Regulation of the small GTPase Rap1 and extracellular signal-regulated kinases by the costimulatory molecule CTLA-4. *Mol. Cell. Biol.* **25**, 4117–4128 (2005).
43. H. Schneider, E. Valk, S. da Rocha Dias, B. Wei, C. E. Rudd, CTLA-4 up-regulation of lymphocyte function-associated antigen 1 adhesion and clustering as an alternate basis for coreceptor function. *Proc. Natl. Acad. Sci. U.S.A.* **102**, 12861–12866 (2005).
44. D. Bernard *et al*., Costimulatory receptors in a teleost fish: Typical CD28, elusive CTLA4. *J. Immunol.* **176**, 4191–4200 (2006).
45. S. Kaur, O. S. Qureshi, D. M. Sansom, Comparison of the intracellular trafficking itinerary of ctla-4 orthologues. *PLoS One* **8**, e60903 (2013).
46. B. Haastert, R. J. Mellanby, S. M. Anderton, R. A. O'Connor, T cells at the site of autoimmune inflammation show increased potential for trogocytosis. *PLoS One* **8**, e81404 (2013).
47. B. Akkaya *et al*., Regulatory T cells mediate specific suppression by depleting peptide-MHC class II from dendritic cells. *Nat. Immunol.* **20**, 218–231 (2019).
48. T. Takahashi *et al*., Immunologic self-tolerance maintained by CD25+CD4+ naturally anergic and suppressive T cells: Induction of autoimmune disease by breaking their anergic/suppressive state. *Int. Immunol.* **10**, 1969–1980 (1998).
49. S. C. Garrett-Thomson *et al*., Mechanistic dissection of the PD-L1:B7-1 co-inhibitory immune complex. *PLoS One* **15**, e0233578 (2020).
50. S. C. Wei *et al*., Combination anti-CTLA-4 plus anti-PD-1 checkpoint blockade utilizes cellular mechanisms partially distinct from monotherapies. *Proc. Natl. Acad. Sci. U.S.A.* **116**, 22699–22709 (2019).
51. A. Cossarizza *et al*., Guidelines for the use of flow cytometry and cell sorting in immunological studies (second edition). *Eur. J. Immunol.* **49**, 1457–1973 (2019).
52. M. Ono *et al*., Foxp3 controls regulatory T-cell function by interacting with AML1/Runx1. *Nature* **446**, 685–689 (2007).